

## SOLVOLYSIS LIQUEFACTION AND CHARACTERIZATION OF BIOPOLYOL PREPARED FROM LIQUEFIED OIL PALM FRUIT WASTE

S. Kormin, A. Z. M. Rus\* and M. S. M. Azahari

Sustainable Polymer Engineering, Advanced Manufacturing and Material Center  
(SPEN-AMMC), Faculty of Mechanical and Manufacturing Engineering, Universiti Tun  
Hussein Onn Malaysia, 86400 Batu Pahat, Johor, Malaysia

Published online: 1 February 2018

### ABSTRACT

From our previous paper, the optimal liquefaction conditions for biopolyol production were determined to be PW/ PEG400 = 1/3, 5% (w/w) acid loading and liquefaction at 150°C for 120 min. Studies on their thermal properties were carried out by thermogravimetry analyzer (TGA). Chemical properties of each PW fibre and liquefied PW residue were investigated by X-ray diffraction analysis (XRD). The Fourier transform-infrared (FT-IR) were selected to analyze the functional group of PW fibre and liquefied PW residue. Liquefied PW residue had higher weight loss percent and lower residual ratios. In other word, the thermal stabilities of liquefaction residue decreased in TGA analysis. FT-IR of the PW fibre and liquefied PW biopolyol fraction confirmed the formation of larger amounts of long-chain lipophilic compounds under liquefaction conditions.

**Keywords:** oil palm fruit waste; solvolysis; liquefaction; biopolyol.

Author Correspondence, e-mail: [zafiah@uthm.edu.my](mailto:zafiah@uthm.edu.my)

doi: <http://dx.doi.org/10.4314/jfas.v10i2s.52>



## 1. INTRODUCTION

Lignocellulosic biomass is the world's fourth largest energy source worldwide, following coal, oil and natural gas. Theoretically, biomass has the capacity to provide 100% of the world's energy requirement. Thermochemical conversion (TCC) technologies have been studied as early as the 17th century by Lawrence Berkeley for his work in the lignocellulosic biomass liquefaction [1]. Lignocellulosic biomass could be liquefied under acid conditions with liquefying reagents such as ethylene glycol and ethylene carbonate to produce polyol products [2]. Liquefying reagents with acid as a catalyst will cause organic material to degrade into smaller molecules by polyhydric alcohols and reform by adding hydrogen ions into the hydrocarbons via solvolytic reactions. Liquefaction of lignocellulosic biomass can be either acid- or base-catalyzed with the former being more common. The main advantage of liquefaction over pyrolysis and gasification is that liquefaction does not require dried biomass as the initial feedstock (drying is an energy-consuming process) [3]. Moreover, liquefaction process occurs under relatively mild conditions when compared to pyrolysis or gasification. Liquefaction reduces the number of unit operations required and effective method for converting lignocellulosic biomass into small fragments that can be used for biochemical, polyol products, etc.[4-5].

Generally, the liquefaction of hemicellulose, lignin, and amorphous cellulose occurs rapidly during the early stages of the liquefaction process because they have amorphous structures that are easily accessible to liquefaction solvents. In contrast, the liquefaction of crystalline cellulose is typically slower and continues through the later stages of the liquefaction process because it has a well-packed molecular structure that is less accessible to the solvents [6]. For this reason, cellulose liquefaction is commonly considered to be the rate-limiting step in the biomass liquefaction process [6-7]. Fig. 1 shows one of the major liquefaction reactions occurring during the acid-catalyzed liquefaction of cellulose. The cellulose is first decomposed by solvolytic reactions into glucose or other small cellulose derivatives that can react with the liquefaction solvent to form glycoside derivatives. Then, the produced glycoside derivatives undergo further reactions to form levulinic acid and/or levulinates [8-9].

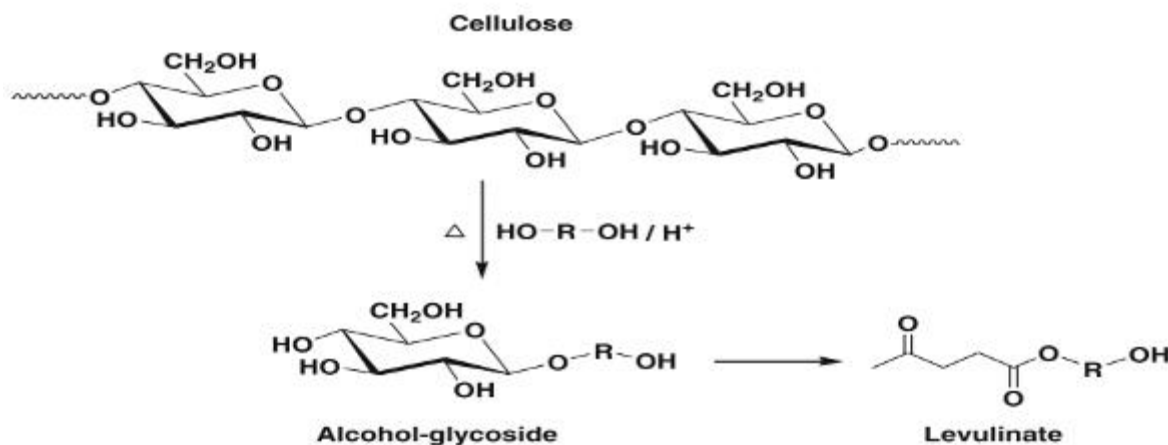


**Fig.1.** Reaction mechanism of acid-catalyzed liquefaction of cellulose in polyhydric alcohols

Polyols are chemical compounds containing multiple hydroxyl groups. The hydroxyl groups of the lignocellulosic biomass make it possible to carry out biopolymer production. Liquefaction is an effective method to convert lignocellulosic biomass into intermediates rich in hydroxyl groups [10-12]. Many researchers have used lignocellulosic biomasses to substitute for fossil resources and to prepare biopolyol products successfully such as corn bran, wood, corn stover and rice straw, wheat straw, bagasse and cotton stalks, lignin, rapeseed cake, olive stone and apple pomace [13-14] have been studied for the production of biopolyols. However, we have not found any report on the comparison of the liquefaction yield of different types of oil palm fruit waste and its residues. Because the lignocellulosic liquefaction process was inconstant, the research on liquefaction reaction of oil palm fruit waste has been insufficient and the formation reasons of the new condensed residues have not yet been ascertained until now.

Therefore, in this present article, we designed the experiments to compare the performance of liquefaction process of different oil palm fruit waste; oil palm mesocarp fibre (PM), oil palm shell (PS) and oil palm kernel (PK) when different reaction condition were used. Generally, the goal of the research presented here was to study further the morphological properties, thermal properties and chemical groups variation in liquefied oil palm fruit waste (PW) products obtained by SEM-EDX, TGA and GCMS respectively. By this work, some basic information can be provided to the study of oil palm fruit waste liquefaction mechanism. The liquefied products were also characterized with FTIR spectra.

## 2. METHODOLOGY

### 2.1. Raw Materials

Oil palm fruit wastes (PW) which contain oil palm mesocarp fibre (PM), oil palm shell (PS) and oil palm kernel (PK) were collected from Sindora Palm oil mills, Johor, Malaysia. The PW were milled into smaller sizes using heavy duty laboratory blender and sieved. The particles of mesh 20-100  $\mu\text{m}$  were selected for the liquefaction experiment. These raw materials were then dried in an oven at 105°C for one night and kept in a desiccator at room temperature to remove moisture content. Polyhydric alcohol (PA) such as polyethylene glycol 400 (PEG400) were used as liquefaction solvents and sulfuric acid (98%) was used as the catalyst. All chemicals used were purchased from Sigma-Aldrich [10].

### 2.2. Liquefaction Oil Palm Fruits Waste (LPW)

Polyethylene glycol 400 (PEG400) was used as the main liquefaction solvent in the experiment. Liquefaction processes were performed using 20g of oven-dried PW fibre and liquefaction solvent were mixed at 1/3 of weight ratio with 5% sulfuric acid as a catalyst. The mixture was placed into a 250 mL three-branch flask in oil bath equipped with thermometer and magnetic stirrer at 150°C for 120 min (2 hours). Then, the flask mixture was immersed in a cold-water bath to stop the reaction process. The liquefied PW were dissolved in 100 mL of methanol for 4 h. The liquefied solutions were then vacuum-filtered and evaporated at 70°C using rotary evaporator to remove the solvent. The obtained black liquid was namely as crude liquefied PW biopolyols. The liquefied PW residue was washed with methanol, dried at 100°C overnight in an oven and weighed [11]. Fig. 2 shows research methodology and experimental setup of solvolysis liquefaction.

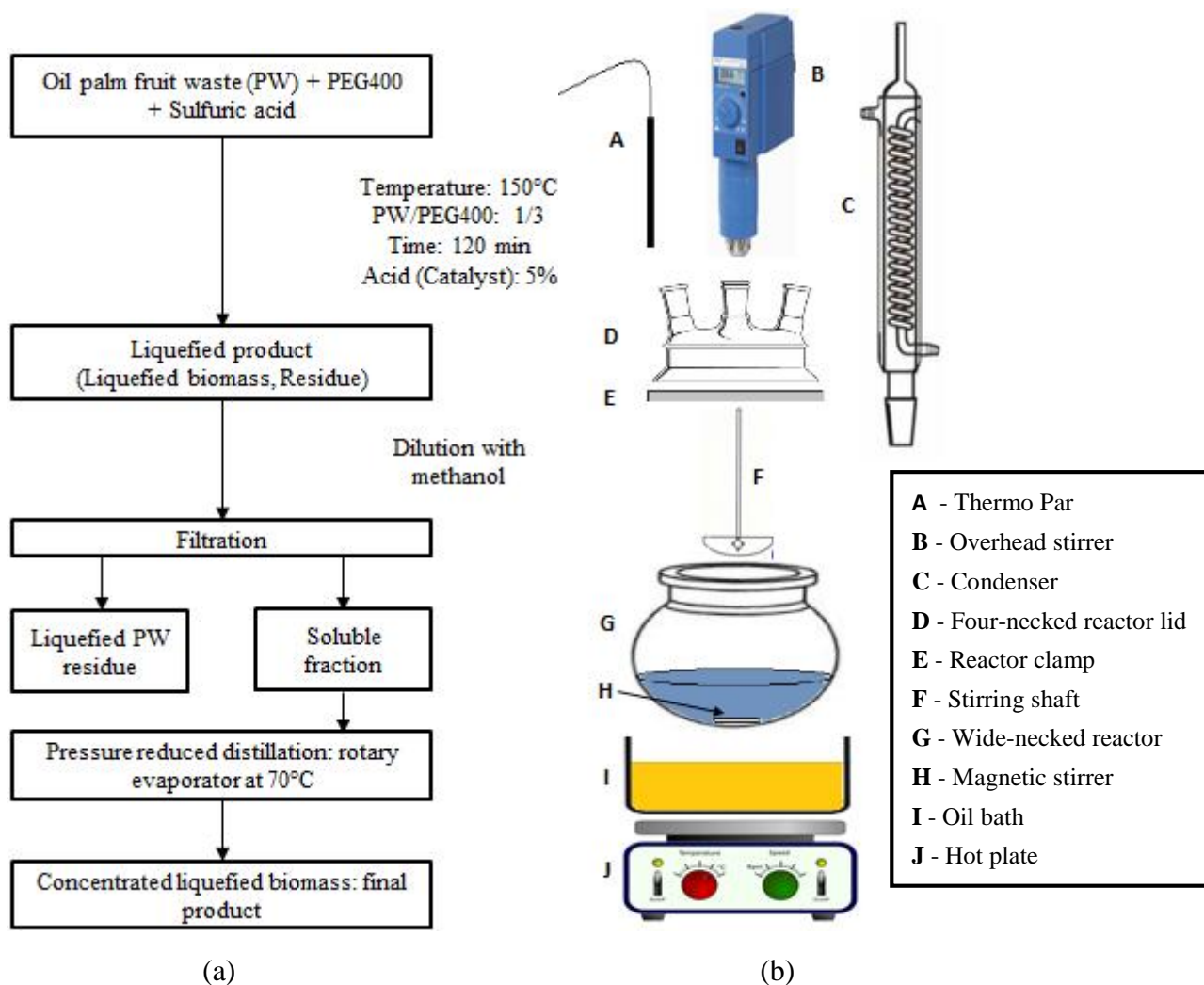


**Fig.2.** Research methodology (a) flow chart (b) experiment setup for solvolysis liquefaction

### 2.3. Thermal Gravimetric Analysis (TGA)

Thermal gravimetric analysis (TGA) and differential thermal analysis (DTA) measurement was performed using Linseis thermogravimetric analyzer for characterized the thermal properties of PW fibre and liquefied PW residue. The TGA was measured the weight loss and derivative weight loss curve. First, 5-8 mg of the sample was placed in an alumina crucible. Then, the samples were heated from 40 to 600 °C at the heating of 10°C/min under oxygen atmosphere, flow rate 0.3 µL [15].

### 2.4. Optical Microscope

The cellular structure of PW fibre and liquefied PW residue was investigated by using industrial microscope with model code 'Eclipse 3x2 LV140' equipped by Nikon (Japan) Corporation. Test preparations were typically done according to the ASTM E2015-04 standards [16]. The optical microscope is able to generate a micrograph of small objects by

means of magnification lenses and visible light, the magnification range of this microscope is 5X-10X.

### 2.5. Scanning Electron Microscope (SEM)

PW fibre and liquefied PW residue surfaces were examined by A JEOL-JSM6380LA Scanning Electron Microscope. The sample was mounted on the holder using double sided tape and sputter-coated with gold to impart electrical conductivity and reduce charging artifacts by using Auto Fined Coater of JEOL-JFC1600. The operation voltage of the SEM was 10kV with 40  $\mu$  v [17].

### 2.6. X-Ray Diffraction Analysis

The degree of crystallinity of the PW fibre and liquefied PW residues was measured by X-ray diffraction. Each sample from different liquefaction conditions were pressed into disks and analyzed with a Bruker D8 Advance X-ray diffractometer. The X-ray diffractograms were performed at 36 kV and 20 mA using nickel-filtered Cu-K (wavelength 1.5405  $\text{\AA}$ ) radiation. The scan was done from 8 $^\circ$  to 40 $^\circ$  with a scanning speed of 0.25 /min and sampling interval of 0.02 $^\circ$ . Jade 5.0 software were used for the peak fitting and phase determination. The biomass crystallinity index (CrI) was defined as the percentage of crystalline material in the biomass and was calculated according to the empirical Segal method [18-19]. The crystallinity index (CrI) of the fibre and residue was calculated using the Segal method from the following equation:

$$CrI = \left( \frac{I_{002} - I_{am}}{I_{002}} \right) \times 100 \quad (1)$$

where  $I_{002}$  is the intensity of the diffraction from the (002) plane at  $2\theta = 22.6^\circ$  and  $I_{am}$  is the intensity of the background scatter measured at  $2\theta = 18.5^\circ$ .

### 2.7. Fourier Transform Infrared (FT-IR) Analysis

The Fourier transform infrared spectroscopy system that was employed in this work was Perkin Elmer spectrometer (Spectrum 100) Universal ATR Sampling Accessory. Liquefied PW biopolyol, fibre and residue were place in FT-IR sample holder. FT-IR spectra were recorded in the range of 600 to 4000  $\text{cm}^{-1}$  collecting 35 scans with 4  $\text{cm}^{-1}$  resolution in the transmittance mode [11].

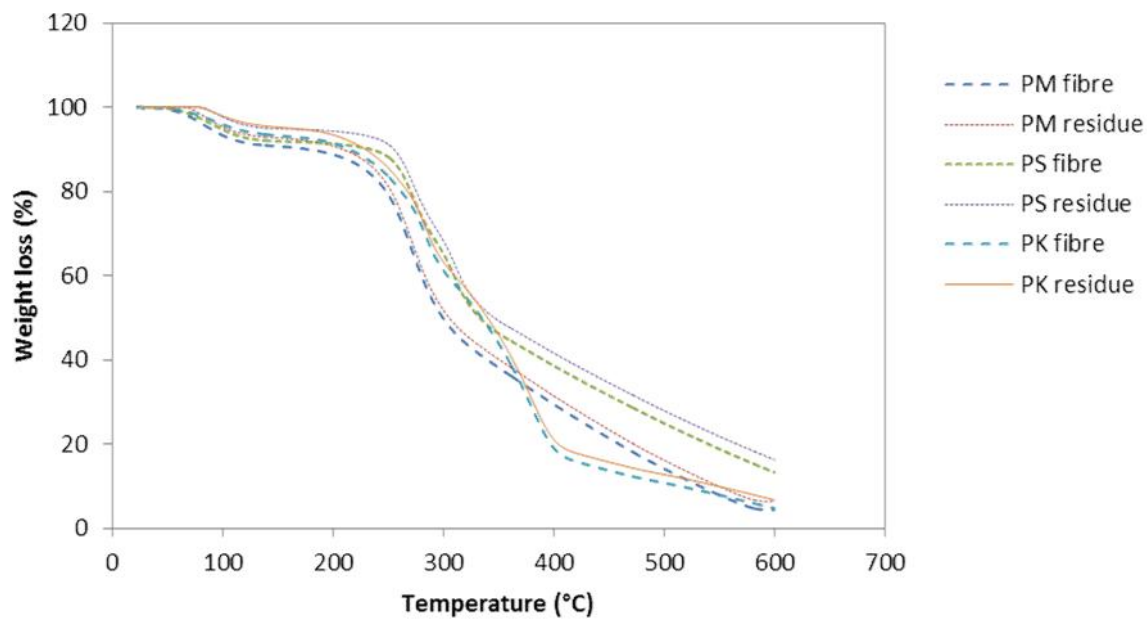
### 3. RESULTS AND DISCUSSION

#### 3.1. Thermogravimetric Analysis (TGA)

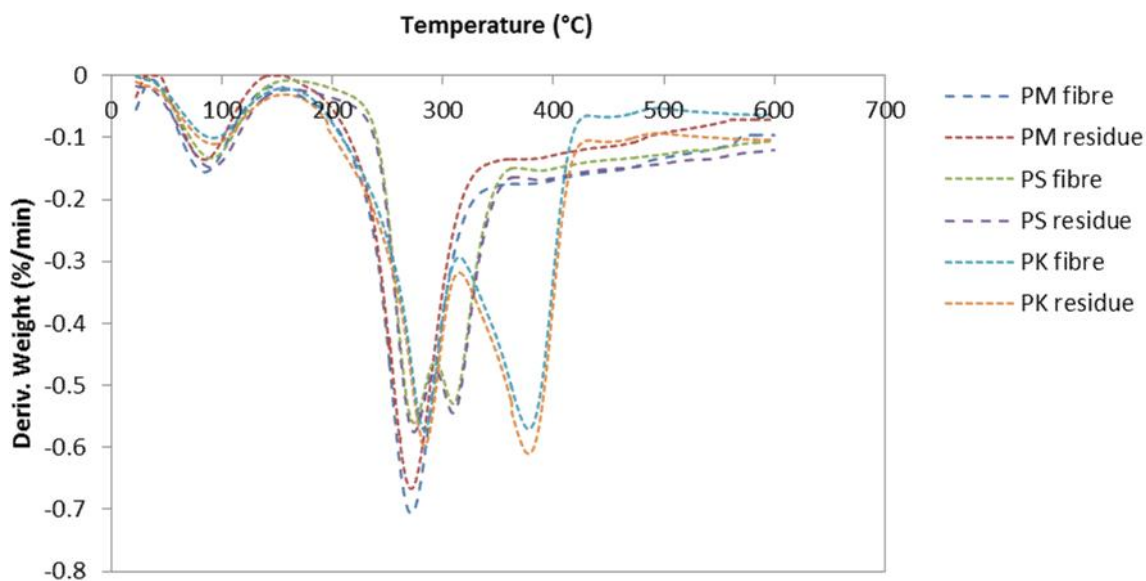
Fig. 3 presents the thermogravimetric (TGA) and derivative weight loss (DTG) curves for oil palm fruit waste (PW) fibres and liquefied PW residue at  $10^{\circ}\text{C}\cdot\text{min}^{-1}$ . The first point degradation correlates with the hard segment while the second peak correlates with the degradation of the soft segment. Qualitative characterization of the degradation process is elaborate by the onset and maximum peak temperature of the first step  $T_{1\text{on}}$  and  $T_{1\text{max}}$  along with the same for second step  $T_{2\text{on}}$  and  $T_{2\text{max}}$ . Detail TGA data, the onset decomposition temperature ( $T_{\text{onset}}$ ) and the maximum decomposition temperature ( $T_{\text{max}}$ ) for PW fibre and liquefied PW residue are tabulated in Table 1. The curves of TGA diagrams which exhibits thermal degradation began to occur only after the materials have absorbed a certain amount of energy. The initial weight lost for PW fibre lignin associated with water evaporation is shown in Fig. 3(a). It is clear that the decomposition of PW fibre and liquefied PW residue is characterized by a very small weight loss at around  $100^{\circ}\text{C}$  attributed to the release of residual water. The second weight lost with temperature between  $200^{\circ}\text{C}$  and  $300^{\circ}\text{C}$  indicated the degradation of hemicelluloses, which attached to lignin structure.

As can be seen, the TGA curves of PM, PS and PK fibre and its residue show three stage of weight loss. These weight losses were attributed to the decomposition of PW fibre and liquefied PW residue respectively. The further weight loss of PM, PS and PK residue up to  $250^{\circ}\text{C}$  could be attributed to the volatilization of methanol. The weight loss percent of PM and PK fibre and its residue increased sharply at  $250^{\circ}\text{C}$ , while the weight loss processes of PS fibre and residue products mainly in the range from  $280^{\circ}\text{C}$ . When the TGA temperature reached over  $500^{\circ}\text{C}$ , the weight loss curve of PW fibre and PW residue remained constant with a residual weight of approximately 15-40% of solid form, non-volatile residue and were not completely burned which consisted mainly of coke and ash [20]. This result reveals that PW fibre lignins are stable at high temperature, which is attributed by the high degree of branching and formation of highly condensed aromatic structure for both types of lignin. This thermal characteristic is reported to be similar to phenol formaldehyde resin [21, 18]. The dramatic difference between the TGA curves of PW fibre and liquefied PW residue suggested that extensive reactions occurred among the components of biomass fibre during the

production process of liquefied biopolyols.



(a)



(b)

**Fig.3.** Overlay thermogravimetry (TGA) (a) differential thermogravimetry (DTG) (b) and differential thermal analysis (DTA) (c) of PW fibre and liquefied PW residue

**Table 1.** Thermal decomposition of PW fibre and liquefied PW residue at 10°C/min

| Samples                   | PM    | PM      | PS    | PS      | PK    | PK      |
|---------------------------|-------|---------|-------|---------|-------|---------|
|                           | Fibre | Residue | Fibre | Residue | Fibre | Residue |
| First Decomposition (°C)  | 232   | 229     | 104   | 102     | 230   | 227     |
| T <sub>1on</sub> (°C)     | 93    | 86      | 93    | 87      | 91    | 85      |
| T <sub>1max</sub> (°C)    | 290   | 287     | 210   | 207     | 288   | 284     |
| Weight loss (%)           | 29    | 31      | 7     | 9       | 28    | 30      |
| Second Decomposition (°C) | 314   | 301     | 226   | 219     | 312   | 299     |
| T <sub>2on</sub> (°C)     | 290   | 288     | 210   | 207     | 288   | 284     |
| T <sub>2max</sub> (°C)    | 395   | 386     | 307   | 302     | 393   | 385     |
| Weight loss (%)           | 51    | 53      | 39    | 41      | 49    | 51      |
| Third Decomposition (°C)  | 410   | 402     | 311   | 305     | 409   | 399     |
| T <sub>3on</sub> (°C)     | 395   | 383     | 307   | 302     | 393   | 385     |
| T <sub>3max</sub> (°C)    | 596   | 594     | 596   | 594     | 593   | 592     |
| Weight loss (%)           | 18    | 20      | 35    | 37      | 17    | 19      |

Fig. 3(b) illustrates the DTG profiles of oil palm fruit waste (PW) fibres and liquefied PW residue at 10°C.min<sup>-1</sup>. TGA curves indicate the weight loss of PW samples in relation to the temperature of thermal degradation, while the first derivative of that curve (DTG) shows the corresponding rate of weight loss. The peak of this curve (DTG<sub>max</sub>) is expressed as a single thermal decomposition temperature and can be used to express the thermal stability characteristics for any materials. From the DTG profiles, there were obvious differences among PW fibre and liquefied PW residue. Only one sharp peak occurred on the DTG curve of PM fibre and its residue after 200°C. However, two peaks appeared on the curves of the PS, PK fibre and its residue. Both were higher than 200°C. The DTG peak from PM fibre and its residue was the highest, the corresponding peak from condensed PS fibre and its residue was the lowest among all the samples which was in the agreement with the results of weight loss percent analyses, suggesting that condensed PS fibre and its residue were harder to be decomposed in TGA because of their special molecular structure [22]. The DTG peak of PM fibre and its residue appeared at lower temperature zone, while the peaks of PS, PK fibre and

its residue distributed at higher temperature zone. DTG profile is a result of differential calculation for TGA data, so the higher peak stands for higher weight loss rate. The difference of DTG profiles between PW fibres and liquefied PW residue indicated that the temperature at which weight loss rate was up to the maximum became higher after liquefaction process [23]. The intense peaks at 290°C and 350°C in DTG curves are attributed to the hemicellulose and cellulose decomposition respectively.

### 3.2. Optical Microscope (OM) and Scanning Electron Microscope (SEM)

The optimum liquefaction condition was obtained at liquefied PW biopolyol was chosen from the previous experiment. The PW particles that remained after liquefaction were analyzed using optical microscope and SEM. The optical micrograph and SEM images of the PW fibre and liquefied PW residue prior to the reaction after the liquefaction reaction process with X100 magnification are shown in Fig. 4. During the reaction, the smallest particles and damaged fibres would undergo dissolution first, leaving behind only the most resistant undamaged parts of the PW fibre. The micrographs reveal a substantial difference in composition and size [24]. Between the tree different PW fibre, there is no so much difference in the residue, that can be explained by the fact that the yield of the reaction is very similar between them. From Fig. 4, PM, PS and PK fibres surface is clearly seen, appear rough and also small fraction of cell wall element can be observed in fibres due to the milling processes [6]. The raw material of PM fibre is very well organized and long compact fibre bundles. PS and PK fibre raw material show compact structure with some impurities were found embedded on the fibre surface. The surface of PK fibre appear oily and compact structure compare to other fibre raw material.

The starting material consisted in PW fibre constituted by a mix of small particles, torn fibres and intact fibre parts. The liquefied PW residue appears to contain only irregular, powdery particles of fibre fragments that occur towards the end of the liquefaction processes. The residue size treated with solvolysis liquefaction is significantly smaller in size compared to the raw materials of PW fibre. It indicated that the rigid fibre bundles cracked into small irregular fragments during liquefaction process. The liquefied PM and PS residue surface has longer fibrous appearance than liquefied PS residue with contains fibre and smaller particles composition materials. Many granules appeared on the surface of liquefied PM and PS

residue, while the liquefied PK residue showed a relative glossy fibre-shaped texture and has more compact structure [19]. The surface of liquefied PM and PS residue is rough and many small fragments of cell wall components are present due to the mechanical processing. As seen, most small fragments attached on the surface of the liquefied PK residue fibres have been removed but the liquefied PM and PS residue mostly remained in its original fibre bundles.

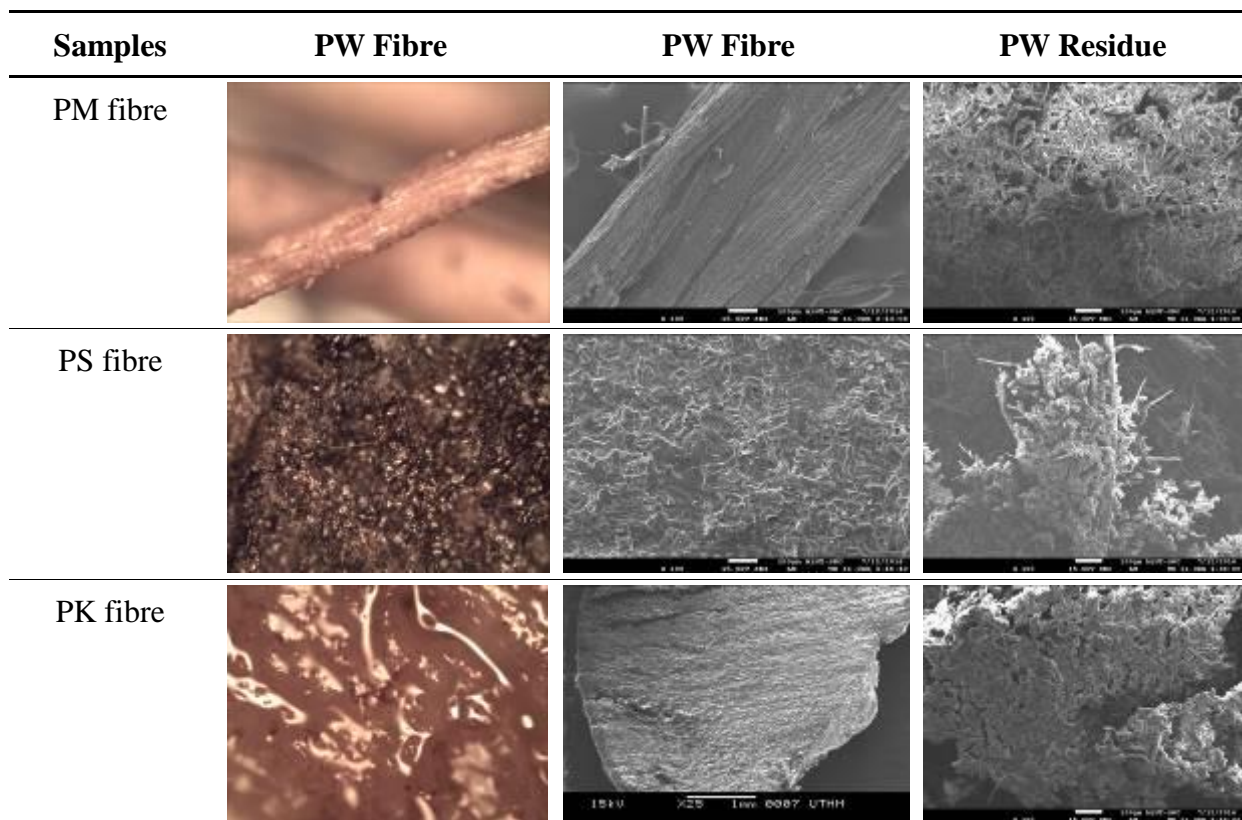


**Fig.4.** Surface morphology of oil palm fruit fibre before and after liquefaction. (a) PM (b) PS (c) PK. Reaction condition: Oil palm mesocarp fibre/liquefaction solvent ratio, 1/3; temperature, 150°C; reaction time, 120 min; biomass loading, 20g; acid loading, 5%

The biomass fibre started to break down to reduce the size of the fibre bundles mainly because the chemical penetration in the longitudinal direction. Eventually, the fibre were broken down to individual fibres because the lignin which works as the binding and supporting material in the middle lamella in fibre tissue had been gradually removed, starting from the outer layer and progressing to inside of the fibre [18]. These results also correspond well with that of the chemical analyses and X-ray diffraction. The small particles are probably

the surface deposits of minerals residues after the liquefaction of lignocellulosic components [19]. In the images with X100 magnification is that the PW fibre particles are really much smaller after carry out the reaction with a PEG400 of liquefaction solvent. With more magnification, it is possible to see that the fibre particles are much more degraded with liquefaction solvent. The degree of depolymerization of PM fibre was substantially higher than with PS and PK fibre.

### 3.3. X-Ray Diffractogram (XRD)

The crystallinity can be used to explain in detail the conversion progress for the amounts of lattice cellulose in oil palm fruit waste (PW). We measured the XRD pattern of cellulose in PW fibre and liquefied PW residue after solvolysis liquefaction. Careful assignment of all the observed X-ray diffraction peaks has been conducted using a diffraction peak-fitting program of Jade 5.0 software. Fig. 5 shows the XRD results for PW fibre and liquefied PW residue. From this figure, we can observe that the shape of the 002 peak at  $2\theta = 22.6^\circ$  in all samples are asymmetric. The peak observed around  $22.6^\circ$  and  $34.6^\circ$  is assigned to the formation of oxidizable lignin. A sharp peak can also be observed around  $\sim 26^\circ$  which is attributed to the formation of carbonaceous structure [25-26]. Accordingly, the CrI of the PW fibre and liquefied PW residue are listed in Table 2 and the CrI of cellulose have been determined.

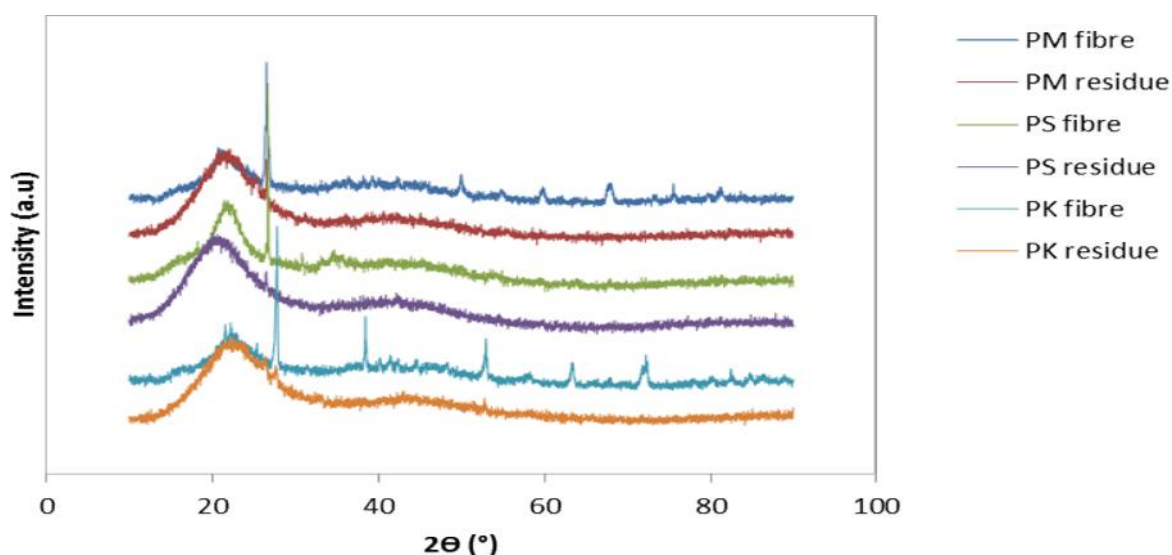


**Fig.5.** X-ray diffractogram (XRD) patterns of PW fibre and liquefied PW residue. Reaction condition: Oil palm fruit waste/liquefaction solvent ratio, 1/3; temperature, 150°C; reaction time, 120 min; liquefaction solvent, PEG400; acid concentration, 5%

Comparing the XRD patterns of PW fibre and liquefied PW residue show the natural occurring cellulose form known as cellulose I. It was reported that the peak at about  $2\theta = 23^\circ$  is the peak for the crystalline portion of biomass (i.e., cellulose) and the peak at about  $2\theta = 18^\circ$  corresponds to the amorphous region [25]. It can be seen that the diffraction peak at  $23^\circ$  (002) is wide and broad for liquefied PW residue. However, the peak was sharper and narrower in PW fibres, hence indicating a higher degree of crystallinity in the PW fibres. Meanwhile, mineral matter such as quartz and calcium sulfate, constituted in all samples. This indicates sufficient liquefaction of the lignocellulose components in the solvolysis liquefaction process. The main components in the ashes of PW residue are silicon dioxide, potassium/sodium oxide and calcium oxide according to reports [19]. Obviously, quartz in the residue is derived from the naturally present  $\text{SiO}_2$  in PW. Previous study shows that CrI of lignocellulosic materials will increase after liquefaction process. The same result can be observed in this research which the phase constitutes contained is shown in Table 3. Liquefaction of lignocellulosic normally carried out in the presence of  $\text{H}_2\text{SO}_4$  as a catalyst. The presence of this acid will enhance the degradation process of cellulosic materials due to the hydrolytic cleavage of polymer glycosidic linkage within nearby molecule hence increase the crystallinity index [7, 27]. Moreover, the increasing of these CrI also affected by the removal of lignin from the amorphous region thus resulting in the relative portion of the crystalline region of cellulose increased [19, 25].

**Table 2.** Crystallinity index of PW fibre and liquefied PW residue

| Sample     | $I_{002}$ | $I_{AM}$ | Crystallinity Index (CrI, %) |
|------------|-----------|----------|------------------------------|
| PM fibre   | 950       | 710      | 25.26                        |
| PM residue | 1450      | 1050     | 27.58                        |
| PS fibre   | 1420      | 900      | 13.33                        |
| PS residue | 1500      | 1300     | 36.62                        |
| PK fibre   | 940       | 740      | 20.00                        |
| PK residue | 1400      | 1120     | 21.28                        |

**Table 3.** Crystal component assignment for XRD

| Sample     | Main Component | Crystallinity Index (CrI, %)   |
|------------|----------------|--------------------------------|
| PM fibre   | Cellulose I    | 22.823, 34.861                 |
|            | Gypsum         | 21.033, 29.067                 |
| PM residue | Cellulose I    | 22.833, 34.841                 |
|            | Gypsum         | 21.123, 29.107                 |
|            | Quartz         | 21.112, 26.662                 |
| PS fibre   | Cellulose I    | 22.820, 34.816                 |
|            | Gypsum         | 21.043, 29.055                 |
| PS residue | Cellulose I    | 22.812, 34.675                 |
|            | Quartz         | 21.110, 26.678                 |
| PK fibre   | Cellulose I    | 22.843, 34.726                 |
|            | Gypsum         | 21.063, 29.062                 |
|            | Quartz         | 21.132, 26.667                 |
|            | Anhydrite      | 25.323, 30.972, 36.321, 38.573 |
| PK residue | Cellulose I    | 22.853, 34.822                 |
|            | Quartz         | 21.122, 26.675                 |

The X-ray crystallinity index (CrI) of the PW fibre and PW residue are listed in Table 3. In general, the CrI of the liquefied PW residue is higher than that of the PW fibre. The crystallinity index for PM, PS and PK was 25.26%, 13.3%, 20.0% and this increased to 27.26%, 36.62% and 21.28% after liquefaction process at a temperature of 150°C for 2 h. The increased of crystallinity in treated samples can be attributed to the removal of cementing amorphous component, which was hemicellulose and a cellulose rich residue was then produced. This result was expected because part of the lignin was removed from the amorphous region of the liquefied PW residue during the liquefaction process. Similar results have been also reported in previous investigations [28]. It is important to note that the CrI is used to indicate the relative, rather than the absolute, amount of the crystalline region in cellulose. Therefore, when the lignin in the amorphous region decreased, the relative portion of the crystalline region of cellulose increased. A similar result has also been found by other

researchers [29-31]. Fibre with high crystallinity might improve the mechanical properties of the composite. It will promote the resistance to cracks which may contribute to better mechanical properties. After the liquefaction, the hydrogen bonds between cellulose molecules resulted in an ordered system. Individual fibrillar units consist of long periods of ordered regions interrupted by completely disordered regions [25].

### 3.4. Fourier Transform Infrared (FT-IR) Analysis

Fig. 6 shows the FT-IR absorption spectrum for the PW fibre, liquefied PW biopolyol and residue with PEG400 at 150°C in the presence of 5% H<sub>2</sub>SO<sub>4</sub> as catalyst. The spectra were recorded in the range of 600 to 4000 cm<sup>-1</sup>. The FT-IR spectra were separated into two information-rich regions: strong and prominent stretching vibration modes in the 3800 to 2800 cm<sup>-1</sup> region and the fingerprint region at 1800 to 800 cm<sup>-1</sup>. FT-IR spectra of PW fibre (PM, PS and PK fibre) raw materials are complex due to the various functional groups and the complicated chemical environment that exist in PW components. FT-IR spectra of PW fibre, liquefied PW biopolyol and residue did show some differences between each other which most of the peaks in IR spectra are broad and often overlap with neighboring peaks.

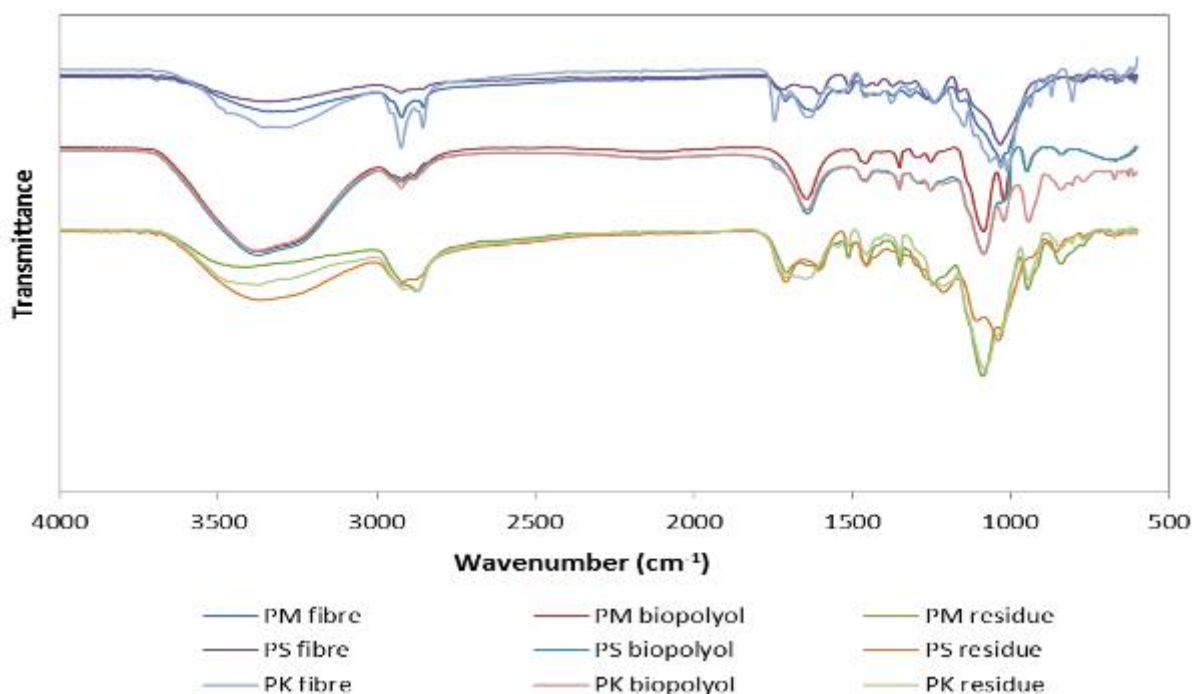


**Fig.6.** FT-IR spectra of PW fibre and fractionated liquefied PW product: Reaction condition: Oil palm fruit waste/liquefaction solvent ratio, 1/3; temperature, 150°C; reaction time, 120 min; liquefaction solvent, PEG400; acid concentration, 5%

A broad peak around 3000 to 3400  $\text{cm}^{-1}$  attributed to OH groups stretching absorption either from cellulose or from unreacted liquefaction solvent in PW fibre, biopolyol and residue. It also due to the H bonded OH groups and the stretching frequency of the OH group as well as intramolecular and intermolecular hydrogen bonds [32]. The OH stretching vibration at 3300 to 3310  $\text{cm}^{-1}$  and the C-H stretching vibration at 2870 to 2920  $\text{cm}^{-1}$  in the 2800 to 3800  $\text{cm}^{-1}$  region are common to all the chemical components [10]. The stretching vibration of N-H bonds at 3300 to 3500  $\text{cm}^{-1}$  can overlap OH group which belong to the water or PW biopolyol. The peak around 2800 to 2990  $\text{cm}^{-1}$  represents the C-H symmetric stretching in aliphatic methyl. The high extent of the reaction for the C-H stretching modes of the aliphatic  $\text{CH}_3$ ,  $\text{CH}_2$  and CH groups is due to the rupture in the chemical backbone of the biomass and the functionalization of free hydroxyl groups in cellulose, lignin and hemicellulose [33-34].

A shoulder at 1735  $\text{cm}^{-1}$  is primarily due to the carbonyl stretch in unconjugated ketone, ester or carboxylic groups in hemicelluloses. Additionally, the increase in the peak intensity of methyl groups was probably due to two reasons, one reason was that the bonds between the coupling of benzene ring units ruptured and smaller benzene ring units formed, the other was that the alkylation reaction of the phenol hydroxyl units of the lignin occurred [35]. All the above results indicated that oxypropylation and liquefaction processes induced a successful chain extension reaction for the conversion of PW fibre into polyols and residue. The peak at 1720 to 1740  $\text{cm}^{-1}$  was assigned to C=O stretching vibration of the carboxyl and acetyl groups in hemicellulose. The peak spectra attributed to the stretching vibration of C=O in hemicelluloses or stretching vibration of carbonyl resulted from cellulose degradation, corresponding with the fact that lignocellulosic biomass liquefaction in presence of acid leads to decomposition of cellulose into small compounds due acid hydrolysis and other oxidation reactions takes place on cellulose [28]. These esters were probably produced by a dehydration reaction between carboxyl groups of PW components in presence of the acid (catalyst). From the growing shoulder of the 1735  $\text{cm}^{-1}$  peak, it can be inferred that hemicellulose is peeled off from adjacent lignin or cellulose into solution. The absorption peaks at 1500 to 1590  $\text{cm}^{-1}$  are attributed to the stretching of the aromatic rings in lignin. The absorption peak at 700 to 900  $\text{cm}^{-1}$  is attributed to the stretching of glycosidic bond in cellulose [12, 36].

As can be seen, the appearance of absorption peak at 1720 to 1740  $\text{cm}^{-1}$  (C=O), 1500 to 1590

$\text{cm}^{-1}$  (N=H) and 1000 to 1200  $\text{cm}^{-1}$  (C-O) had confirmed the formation of urethane linkages as expected. There was no significant difference between the transmittance spectra of the samples [37]. The results indicated that the chemical structures of the samples from the three portions (PW fibre, biopolyol and residue) were the same. However, this does not mean that the effect of differences in chemical structure should be overlooked when comparing the liquefaction of PM, PS and PK fibre. After the solvolysis liquefaction, most of the lignocellulosic peaks of the PW fibre have significantly modified, revealing the decomposition of hemicelluloses, cellulose and lignin components.

#### **4. CONCLUSION**

In conclusion, significant differences in physical, chemical and morphological properties oil palm waste fibre (PM, PS and PK) were observed conventional solvolysis liquefaction products and residues. Oil palm waste fibre was liquefied by using a solvent mixture consisting of PEG 400 with 5% sulfuric acid as catalyst at 150°C for 120 min. This liquefied PW biopolyol could be used as one of the raw materials for preparing value added bio-products such as polyurethane foams. Liquefied PW biopolyols were generated from the solvolysis liquefaction and the lignin derivatives in the crude PW biopolyols were successfully removed by the addition of water as evidenced by FT-IR analyses. FT-IR of the liquefied biopolyol products resulting conventional liquefaction induced intense oxidation cleavage of the lignocellulose biomass and more extensive solvolysis reaction. The XRD patterns indicate that crystalline cellulose is the main resistance to solvolysis liquefaction and it dissolved entirely in conventional liquefaction. Many granules on the surface of the fibre residue demonstrate the acceleration mechanism of the solvolysis liquefaction. The behaviour of the obtained liquefied biopolyol showed acceptable quality and will be further studied in order to be used in the preparation of PU foams production.

#### **5. ACKNOWLEDGEMENTS**

The author would like to thanks Sustainable Polymer Engineering, Advanced manufacturing and materials Center (SPEN-AMMC), Universiti Tun Hussein Onn Malaysia (UTHM), Johor and Centre for Graduate Studies UTHM for supporting this research.

## 6. REFERENCES

- [1] Christensen P S. Hydrothermal liquefaction of waste biomass: Optimizing reaction parameters. PhD thesis, Denmark: Aarhus University, 2014
- [2] Mazaheri H, Lee K T, Bhatia S, Mohamed A R. Sub/supercritical liquefaction of oil palm fruit press fiber for the production of bio-oil: Effect of solvents. *Bioresource Technology*, 2010, 101(19):7641-7647
- [3] Patel M, Zhang X, Kumar A. Techno-economic and life cycle assessment on lignocellulosic biomass thermochemical conversion technologies: A review. *Renewable and Sustainable Energy Reviews*, 2016, 53:1486-1499
- [4] Pan H. Synthesis of polymers from organic solvent liquefied biomass: A review. *Renewable and Sustainable Energy Reviews*, 2011, 15(7):3454-3463
- [5] Xue B L, Wen J L, Sun R C. Producing lignin-based polyols through microwave-assisted liquefaction for rigid polyurethane foam production. *Materials*, 2015, 8(2):586-599
- [6] Li Y., Luo X., Hu S. *Bio-based polyols and polyurethanes*. Cham: Springer, 2015
- [7] Ramsurn H. Gasification, liquefaction and deoxy-liquefaction of switchgrass using sub-and supercritical water. PhD thesis, Alabama: Auburn University, 2013
- [8] Xiao W, Pang A, Wang X, Liu J, Han L. Separation and analysis of microwave-assisted liquefied products of corn stover. *BioResources*, 2014, 9(4):7109-7118
- [9] Caillol S, Desroches M, Boutevin G, Loubat C, Auvergne R, Boutevin B. Synthesis of new polyester polyols from epoxidized vegetable oils and biobased acids. *European Journal of Lipid Science and Technology*, 2012, 114(12):1447-1459
- [10] Kormin S, Rus M, Zafiah A. Preparation and characterization of biopolyol from liquefied oil palm fruit waste: Part 1. In *7th International Conference on Manufacturing Science and Technology*, 2016, pp. 65-69
- [11] Kormin S, Rus M, Zafiah A. Preparation and characterization of biopolyol from liquefied oil palm fruit waste: Part 2. In *7th International Conference on Manufacturing Science and Technology*, 2016, pp. 70-77
- [12] Liang L, Mao Z, Li Y, Wan C, Wang T, Zhang L, Zhang L. Liquefaction of crop residues for polyol production. *BioResources*, 2007, 1(2):248-256
- [13] Mohammed A A. Investigation of tensile and impact of composite materials reinforced

with natural materials. *Engineering and Technology Journal*, 2015, 33(4):919-933

[14] Bujang A S. Utilization of durian biomass for biorenewable applications. PhD thesis, Ames: Iowa State University, 2014

[15] Hassan N N. Thermal characteristic of biopolymer foam using hot compression technique. In *Malaysia University Conference Engineering Technology*, 2014, pp. 10-11

[16] Bakri M K, Jayamani E, Heng S K, Hamdan S. Reinforced oil palm fiber epoxy composites: An investigation on chemical treatment of fibers on acoustical, morphological, mechanical and spectral properties. *Materials Today: Proceedings*, 2015, 2(4-5):2747-2756

[17] Adnan N Q, Rus M, Zafiah A. Sound absorption of laminated biopolymer foam and epoxy foam. *Key Engineering Materials*, 2013, 594-595:291-295

[18] Pan H. Wood liquefaction in the presence of phenol with a weak acid catalyst and its potential for novolac type wood adhesives. PhD thesis, Baton Rouge: Louisiana State University, 2007

[19] Xiao W, Han L, Zhao Y. Comparative study of conventional and microwave-assisted liquefaction of corn stover in ethylene glycol. *Industrial Crops and Products*, 2011, 34(3):1602-1606

[20] Ibrahim M N, Zakaria N, Sipaut C S, Sulaiman O, Hashim R. Chemical and thermal properties of lignins from oil palm biomass as a substitute for phenol in a phenol formaldehyde resin production. *Carbohydrate Polymers*, 2011, 86(1):112-119

[21] Yip J, Chen M, Szeto Y S, Yan S. Comparative study of liquefaction process and liquefied products from bamboo using different organic solvents. *Bioresource Technology*, 2009, 100(24):6674-6678

[22] Niu M, Zhao G J, Alma M H. Thermogravimetric studies on condensed wood residues in polyhydric alcohols liquefaction. *BioResources*, 2011, 6(1):615-630

[23] Niu M, Zhao G, Alma M. FT-IR and TGA studies on liquified wood products in the condensation reaction process. *Wood Research*, 2011, 56(2):221-232

[24] Vivekanandhan S, Zarrinbakhsh N, Misra M, Mohanty A K. Coproducts of biofuel industries in value-added biomaterials uses: A move towards a sustainable bioeconomy. In Z. Fang (Ed.), *Liquid, gaseous and solid biofuels-conversion techniques*. Rijeka: Intech, 2013, pp. 491-541

- [25] Nordin N I, Ariffin H, Andou Y, Hassan M A, Shirai Y, Nishida H, Yunus W M, Karuppuchamy S, Ibrahim N A. Modification of oil palm mesocarp fiber characteristics using superheated steam treatment. *Molecules*, 2013, 18(8):9132-9146
- [26] Midgett J S. Assessing a hydrothermal liquefaction process using biomass feedstocks. Master thesis, Baton Rouge: Louisiana State University, 2008
- [27] Acero N F. Polyurethane foams from renewable and sustainable polyols. Master thesis, Lisbon: Instituto Superior Tecnico. 2014
- [28] Briones R, Serrano L, Llano-Ponte R, Labidi J. Polyols obtained from solvolysis liquefaction of biodiesel production solid residues. *Chemical Engineering Journal*, 2011, 175:169-75
- [29] Pan H, Hse C Y, Shupe T F. Wood liquefaction and its application to novolac resin. 2009, <https://pdfs.semanticscholar.org/f0c0/d04a3ca494d6f7e427fdb8e2285d1e8cfb62.pdf>
- [30] Chen Y, Wu Y, Zhang P, Hua D, Yang M, Li C, Chen Z, Liu J. Direct liquefaction of *Dunaliella tertiolecta* for bio-oil in sub/supercritical ethanol-water. *Bioresource Technology*, 2012, 124:190-198
- [31] Wei N, Via B K, Wang Y, McDonald T, Auad M L. Liquefaction and substitution of switchgrass (*Panicum virgatum*) based bio-oil into epoxy resins. *Industrial Crops and Products*, 2014, 57:116-123
- [32] Qi J, Xie J, Hse C Y, Shupe T F. Analysis of *Phyllostachys pubescens* bamboo residues for liquefaction: Chemical components, infrared spectroscopy, and thermogravimetry. *BioResources*, 2013, 8(4):5644-5654
- [33] Briones R, Serrano L, Llano-Ponte R, Labidi J. Polyols obtained from solvolysis liquefaction of biodiesel production solid residues. *Chemical Engineering Journal*, 2011, 175:169-175
- [34] Bui N Q, Fongarland P, Rataboul F, Dartiguelongue C, Charon N, Vallée C, Essayem N. FTIR as a simple tool to quantify unconverted lignin from chars in biomass liquefaction process: Application to SC ethanol liquefaction of pine wood. *Fuel Processing Technology*, 2015, 134:378-386
- [35] Xue B L, Wen J L, Xu F, Sun R C. Polyols production by chemical modification of autocatalyzed ethanol water lignin from *Betula alnoides*. *Journal of Applied Polymer Science*,

2013, 129(1):434-442

[36] Xie J, Zhai X, Hse C Y, Shupe T F, Pan H. Polyols from microwave liquefied bagasse and its application to rigid polyurethane foam. *Materials*, 2015, 8(12):8496-8509

[37] Kormin S, Rus A Z, Azahari M S. Preparation of polyurethane foams using liquefied oil palm mesocarp fibre (OPMF) and renewable monomer from waste cooking oil. *AIP Conference Proceedings*, 2017, 1877(1):1-7

**How to cite this article:**

Kormin S, Rus A Z M, Azahari M S M. Solvolysis liquefaction and characterization of biopolyol prepared from liquefied oil palm fruit waste. *J. Fundam. Appl. Sci.*, 2018, 10(2S), 701-721.